Asia Pac. J. Math. 2026 **13**:120

A FRACTIONAL WATERBORNE COMPARTMENTAL MODEL OF THE HEPATITIS E EPIDEMIC IN NAMIBIA'S INFORMAL SETTLEMENTS

ADETAYO SAMUEL EEGUNJOBI*, ONESMUS SHUUNGULA, DAVID IIYAMBO, NEGA CHERE

Department of Mathematics, Statistics and Actuarial Science, Namibia University od Science and Technology, Windhoek, Namibia

*Corresponding author: samdet1@yahoo.com

Abstract. Between December 2017 and February 2020, Namibia experienced its first and largest nationwide hepatitis E virus (HEV) epidemic, with 7,247 cases and 61 deaths concentrated in the informal settlements of Windhoek and the Erongo coast. The maternal case-fatality rate reached 6%, an order of magnitude above the general rate, yet the outbreak has not previously been modelled mechanistically. We formulate and analyse a novel seven-compartment S–E–A–I–I_p–R–W model, posed as a Caputo fractional differential system of order $\alpha \in (0, 1]$ that captures the memory inherent in protracted faecal–oral transmission; the classical model is recovered as $\alpha \to 1$. The structure couples SEIR dynamics to an environmental water reservoir W and resolves asymptomatic (A), symptomatic (I), and pregnant/post-partum (I_p) infectious streams. We prove positivity, boundedness, and local (Matignon) and global (fractional Lyapunov) stability, derive $\mathcal{R}_0$ from the next-generation matrix, characterise the endemic equilibrium, and compute sensitivity indices. Simulations use the Diethelm–Ford–Freed scheme with Namibian parameters. We obtain $\mathcal{R}_0 \approx 2.02$ at $\alpha = 1$, decomposing into direct (1.14) and waterborne (1.77) contributions, confirming environmental dominance; $\mathcal{R}_0$ increases with α, falling to approximately 1.45 at $\alpha = 0.7$. A combined WASH and hygiene-promotion strategy reduces $\mathcal{R}_0$ to approximately 1.03. Because the reservoir saturates at low pathogen density, incremental water measures only postpone infections; only threshold-crossing decontamination $(\mathcal{R}_0 < 1)$ prevents the maternal burden. Environmental decontamination must be the cornerstone of HEV control in Namibia.

2020 Mathematics Subject Classification. 92D30.

Key words and phrases. hepatitis E; Namibia; waterborne disease; basic reproduction number; Caputo fractional derivative; stability analysis; sensitivity analysis; maternal mortality.

1. Introduction

Hepatitis E is an acute, self-limiting liver disease caused by the hepatitis E virus (HEV), an RNA virus transmitted predominantly by the faecal–oral route through water and food contaminated with human faeces [3,4]. In low-resource settings the epidemic genotypes 1 and 2 are responsible for large waterborne outbreaks, while the disease becomes life-threatening in pregnant women, in whom it can

DOI: 10.28924/APJM/13-120

progress to fulminant hepatic failure [5,6]. Globally HEV genotypes 1 and 2 were estimated to cause about 20 million infections, 3.3 million symptomatic cases and tens of thousands of deaths annually in the mid-2000s [6,7].

Namibia, an upper-middle-income but highly unequal country in south-western Africa, illustrates how rapid, unplanned urbanisation can re-create the conditions for epidemic HEV. On 14 December 2017 the Ministry of Health and Social Services declared a hepatitis E outbreak in the Khomas region, which contains the capital, Windhoek. The outbreak grew into a protracted nationwide epidemic: during 14 December 2017–2 February 2020 a total of $7{,}247$ outbreak-associated cases were reported across all 14 regions, the majority (59%) in men and 72% in persons aged 20–39 years [1]. Sixty-one deaths (0.8%) were recorded, including 24 $(39\%$ of all deaths$)$ in pregnant or post-partum women, corresponding to a maternal case-fatality rate of about 6% [1]. Cases clustered overwhelmingly in informal settlements, notably Havana and Goreangab in Windhoek and the Democratic Resettlement Community near Swakopmund where, by government estimate, roughly 40% of urban households live with minimal infrastructure, limited access to piped water and latrines, and where settlement populations grow at 8–15% per year against a national rate near 1.4% [1,2]. The World Health Organization and partners emphasised that safe water, improved sanitation, and hygiene (collectively "WASH") were the decisive levers for control, since no HEV vaccine is licensed or available in Namibia [2,8].

Compartmental models remain the standard quantitative tool for understanding transmission, estimating the basic reproduction number $\mathcal{R}_0$ and comparing interventions [9,10,29,37]. For diseases with an environmental reservoir the classical SIR framework is inadequate because it omits the pathogen pool that mediates indirect transmission. Codeço [11] introduced an explicit aquatic-reservoir compartment with a saturating ingestion response for cholera, and Tien and Earn [12] formalised the "$SIWR$" model in which infectious hosts shed pathogen into a water compartment W and acquire infection both directly and through W; they computed $\mathcal{R}_0$, the growth rate and final size, and proved global stability of the endemic equilibrium. Eisenberg, Robertson and Tien [13] studied identifiability of the direct and indirect pathways, a question central to inferring the relative role of water in real outbreaks. These waterborne frameworks were applied with notable success to the 2010 Haitian cholera epidemic [14] and to the 2008–2009 Zimbabwean outbreaks [15], where reproduction numbers and optimal interventions were estimated from surveillance data.

Hepatitis-E-specific models are comparatively scarce. Nannyonga, Sumpter, Mugisha and Luboobi [16] fitted a transmission model to the 2007–2009 Kitgum (Uganda) HEV outbreak, estimated $\mathcal{R}_0 \approx 2.25$, and computed the latrine and borehole coverage required for elimination; they also explored malaria co-infection effects. Ren and colleagues [17] developed a combined statistical–mechanistic model to forecast HEV incidence in Shanghai. More recently, fractional-calculus approaches have been brought to HEV: Osman, Makinde and co-workers [35] modelled zoonotic HEV transmission with a Caputo derivative and a porcine reservoir, while Jena, Chakraverty and Baleanu [36] analysed a time-fractional HEV model with uncertain parameters. Fractional derivatives are attractive for enteric diseases because the Caputo operator endows the system with memory and hereditary properties [24,25], reflecting the long and heterogeneous delays between contamination, ingestion and symptom onset; robust predictor–corrector schemes make such systems numerically tractable [26,27,34].

The literature establishes that (i) environmental reservoir models are essential for waterborne pathogens [11,12]; (ii) HEV behaves as a waterborne epidemic disease in low-WASH settings [7,16]; and (iii) fractional operators improve the description of enteric transmission [35,36]. Three gaps remain. First, *no mechanistic transmission model has been developed for the Namibian HEV epidemic*, despite its size, duration and policy salience. Second, existing HEV models do not isolate the pregnant/post-partum sub-population, even though it carries the overwhelming share of mortality [1,5]; without an explicit I_p class the disproportionate maternal burden cannot be quantified or targeted. Third, the relative contribution of the direct versus waterborne pathway to $\mathcal{R}_0$, the quantity that determines whether hygiene promotion or environmental decontamination should be prioritised has not been estimated for Namibia.

We propose a Caputo *fractional* S–E–A–I–I_p–R–W model (order $\alpha \in (0, 1]$, with the ODE as its $\alpha \to 1$ limit) that (a) embeds an environmental water reservoir with saturating ingestion, (b) resolves a large asymptomatic shedding class alongside the symptomatic classes, and (c) tracks pregnant/post-partum infectives separately with an elevated disease-death rate. We derive a closed-form $\mathcal{R}_0$ that splits additively into direct and waterborne loops, perform a complete stability and sensitivity analysis, and translate the results into WASH-oriented control recommendations specific to Namibia's informal settlements. To our knowledge this is the first such study.

The 2017–2020 epidemic demonstrated that HEV is endemic-prone wherever Namibian urbanisation outpaces sanitation. The disease is preventable, yet it killed disproportionately among pregnant women and persisted for more than two years [1]. Policy responses (water-purification tablets, communal toilet construction, hygiene campaigns) were deployed without a quantitative framework to rank them or to anticipate their effect on transmission and on maternal deaths. There is therefore a concrete need for a mathematically rigorous, data-consistent model that (i) reproduces the qualitative dynamics of a settlement HEV epidemic; (ii) yields a reproduction number whose components map onto the available interventions; (iii) captures the elevated maternal risk; and (iv) is robust to the memory effects characteristic of slow enteric epidemics. Mathematical modelling and numerical investigation are justified because direct experimentation is impossible, surveillance is incomplete, and the counterfactual impact of interventions can only be estimated through a mechanistic model.

Section 2 recalls the fractional-calculus preliminaries. Section 3 formulates the model, states the assumptions, presents the compartmental diagram and the governing equations, and proves positivity and boundedness. Section 4 derives the equilibria, the reproduction number, and the stability results. Section 5 describes the numerical methods, parameter estimation and sensitivity methodology. Section 6 presents and discusses the numerical results and the policy implications, and Section 7 concludes.

2. Preliminaries

We briefly recall the Caputo fractional operator used in the fractional version of the model [24,25].

Definition 2.1 (Caputo fractional derivative)**.** For $\alpha \in (n-1, n]$, $n \in \mathbb{N}$, and $f \in C^n[0,\infty)$, the Caputo derivative of order α is

$$ {}^{C}D_t^{\alpha} f(t) = \frac{1}{\Gamma(n-\alpha)} \int_0^t (t-\tau)^{n-\alpha-1} f^{(n)}(\tau)\,\mathrm{d}\tau. \tag{1}$$

Definition 2.2 (Riemann–Liouville integral)**.** The fractional integral of order $\alpha > 0$ is $I^{\alpha} f(t) = \frac{1}{\Gamma(\alpha)} \int_0^t (t-\tau)^{\alpha-1} f(\tau)\,\mathrm{d}\tau$.

Lemma 2.3 ([27])**.** *Let $0 < \alpha \le 1$ and let $g : \mathbb{R}_+ \times \mathbb{R}^m \to \mathbb{R}^m$ be continuous and Lipschitz in its second argument on a closed region containing the initial point. Then the initial-value problem ${}^{C}D_t^{\alpha} x(t) = g(t, x(t))$, $x(0) = x_0$, possesses a unique continuous solution on a maximal interval of existence.*

Lemma 2.4 (Generalized mean-value / positivity, [25])**.** *If $h \in C[0,b]$ and ${}^{C}D_t^{\alpha} h(t) \in C(0,b]$ with $0 < \alpha \le 1$, then $h(t) = h(0) + \frac{1}{\Gamma(\alpha)} {}^{C}D_t^{\alpha} h(\zeta)\, t^{\alpha}$ for some $0 \le \zeta \le t$. Consequently, if ${}^{C}D_t^{\alpha} h(t) \ge 0$ on $(0,b]$ then h is non-decreasing, and if ${}^{C}D_t^{\alpha} h(t) \le 0$ then h is non-increasing.*

Because the model is posed as a fractional system, its local and global stability cannot be read off from the sign of the real parts of eigenvalues or from the classical LaSalle principle. The two results below are the fractional substitutes used throughout Section 4.

Lemma 2.5 (Matignon stability criterion [28,30])**.** *Consider the autonomous Caputo system ${}^{C}D_t^{\alpha} x(t) = g(x(t))$, $\alpha \in (0,1]$, with equilibrium x^* $(g(x^*) = 0)$ and Jacobian $J = Dg(x^*)$. The equilibrium x^* is locally asymptotically stable if and only if every eigenvalue λ_i of J satisfies*

$$ \left|\arg(\lambda_i)\right| > \frac{\alpha\pi}{2}. \tag{2}$$

In particular, any λ_i with $\mathrm{Re}(\lambda_i) < 0$ obeys $|\arg(\lambda_i)| > \pi/2 \ge \alpha\pi/2$, so Hurwitz stability of J implies fractional stability for every $\alpha \in (0,1]$; the admissible stability sector widens *as α decreases.*

Lemma 2.6 (Fractional comparison / Lyapunov lemma [31,32])**.** *Let $x(t) \in \mathbb{R}_+^n$ be a continuously differentiable solution of a Caputo system. Then for any $x_i(t)$ and any equilibrium value $x_i^* > 0$,*

$$ {}^{C}D_t^{\alpha}\left(x_i - x_i^* - x_i^* \ln \frac{x_i}{x_i^*}\right) \le \left(1 - \frac{x_i^*}{x_i}\right) {}^{C}D_t^{\alpha} x_i, \qquad \tfrac{1}{2} {}^{C}D_t^{\alpha} x_i^2 \le x_i\, {}^{C}D_t^{\alpha} x_i. \tag{3}$$

Moreover, if a continuous $V(x) \ge 0$ satisfies $V(x^*) = 0$ and ${}^{C}D_t^{\alpha} V(x(t)) \le 0$ on a positively invariant set, then x^* is stable; if in addition ${}^{C}D_t^{\alpha} V < 0$ for $x \ne x^*$, then x^* is asymptotically stable.

3. Model formulation

The human population at risk (the informal-settlement catchment) of size $N(t)$ is partitioned into six mutually exclusive compartments: susceptible $S(t)$; exposed (latently infected, not yet infectious) $E(t)$; *asymptomatic* infectious shedders $A(t)$; symptomatic infectious general individuals $I(t)$; symptomatic infectious pregnant or post-partum women $I_p(t)$; and recovered/immune $R(t)$, so that

$$N(t) = S(t) + E(t) + A(t) + I(t) + I_p(t) + R(t). \tag{4}$$

A seventh compartment $W(t)$ measures the density of viable HEV in the shared water/environmental reservoir. The asymptomatic class is included because a large fraction of HEV infections are subclinical yet still excrete virus into the environment; omitting them understates the true reservoir contamination and hence the force of infection [5,7]. The model rests on the following biologically motivated assumptions.

Assumption 3.1.

(1) Recruitment into the susceptible class occurs at constant rate Λ (births plus net in-migration into the settlement); $\Lambda = \mu N_0$ at the demographic steady state, where μ is the per-capita natural death rate and N_0 the baseline population. The high in-migration of informal settlements is absorbed into Λ [1].

(2) Infection is acquired by two pathways: *direct* faecal–oral person-to-person contact at rate $\beta_1(\varepsilon A+I+I_p)/N$, in which asymptomatic individuals transmit at reduced relative infectiousness $\varepsilon \in [0,1]$; and *indirect* ingestion of contaminated water with a saturating (Holling type II / Codeço) response $\beta_2 W/(K+W)$, where K is the half-saturation pathogen density [11,12]. The total force of infection is $\lambda(t) = \beta_1 \frac{\varepsilon A+I+I_p}{N} + \beta_2 \frac{W}{K+W}$.

(3) Exposed individuals become infectious after a mean latent period $1/\sigma$. Incident infections split into three streams: a fraction f_A are asymptomatic (entering A), a fraction $f_P \equiv p$ are pregnant/post-partum women (entering I_p), and the remaining $f_I = 1 - f_A - p$ are general symptomatic (entering I).

(4) Asymptomatic individuals clear infection at rate γ_A; symptomatic individuals recover at rate γ. Recovery confers immunity that wanes at rate ρ. Disease-induced death occurs at rate δ for the general symptomatic class and at the substantially higher rate $\delta_p \gg \delta$ for pregnant/post-partum women [1,5]; asymptomatic infection is non-fatal.

(5) The asymptomatic, general and pregnant infectious classes shed virus into the water reservoir at per-capita rates $\alpha_A, \alpha_1, \alpha_2$; the pathogen is removed (decay, dilution, treatment) at rate ξ.

(6) The settlement is well mixed over the modelling horizon; demographic and epidemiological parameters are time-invariant.

Figure 1 depicts the flow structure.

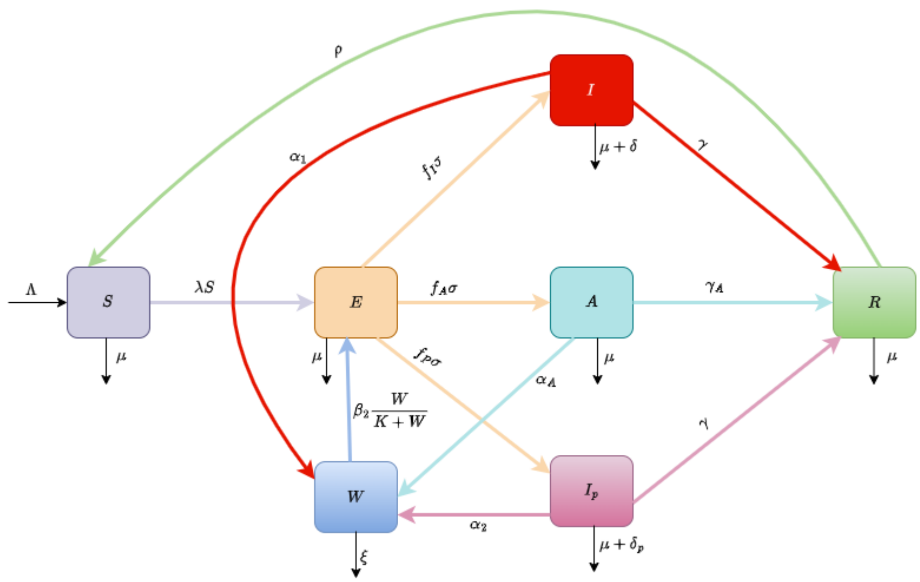

FIGURE 1. Compartmental flow diagram of the Namibian fractional HEV model.

The model is governed by the Caputo fractional system of order $\alpha \in (0, 1]$,

$$ {}^C D_t^\alpha S = \Lambda + \rho R - \lambda S - \mu S, \tag{5a} $$

$$ {}^C D_t^\alpha E = \lambda S - (\sigma + \mu) E, \tag{5b} $$

$$ {}^C D_t^\alpha A = f_A\, \sigma E - (\gamma_A + \mu) A, \tag{5c} $$

$$ {}^C D_t^\alpha I = f_I\, \sigma E - (\gamma + \mu + \delta) I, \tag{5d} $$

$$ {}^C D_t^\alpha I_p = f_P\, \sigma E - (\gamma + \mu + \delta_p) I_p, \tag{5e} $$

$$ {}^C D_t^\alpha R = \gamma_A A + \gamma (I + I_p) - (\rho + \mu) R, \tag{5f} $$

$$ {}^C D_t^\alpha W = \alpha_A A + \alpha_1 I + \alpha_2 I_p - \xi W, \tag{5g} $$

with force of infection $\lambda(t) = \beta_1 \dfrac{\varepsilon A + I + I_p}{N} + \beta_2 \dfrac{W}{K + W}$, incident split $f_I = 1 - f_A - f_P$, $f_P \equiv p$, and biologically meaningful initial conditions

$$ S(0) = S_0 > 0,\ E(0) \ge 0,\ A(0) \ge 0,\ I(0) \ge 0,\ I_p(0) \ge 0,\ R(0) \ge 0,\ W(0) \ge 0. \tag{6} $$

Here ${}^C D_t^\alpha$ is the Caputo derivative of Definition 1. To preserve dimensional homogeneity, since the left hand side carries units of $(\text{time})^{-\alpha}$, every rate constant is raised to the power α. This follows the standard convention used in fractional epidemic models [33,35,36]. The classical integer-order S–E–A–I–I_p–R–W system is recovered *exactly* as the limit $\alpha \to 1$, in which case ${}^C D_t^\alpha \to \mathrm{d}/\mathrm{d}t$ and the powered constants return to their nominal values. Adding the human equations gives

$$ {}^C D_t^\alpha N = \Lambda - \mu N - \delta I - \delta_p I_p \le \Lambda - \mu N, \tag{7} $$

so the total population is fractionally regulated. All variables and parameters are defined in Table 1.

3.1. **Positivity and boundedness.**

Theorem 3.2 (Positivity)**.** *For non-negative initial data* (6) *the solution* (S, E, A, I, I_p, R, W) *of the fractional system* (5) *remains non-negative for all* $t \geq 0$*; the non-negative orthant* $\mathbb{R}^7_+$ *is positively invariant.*

Proof. Evaluate each Caputo derivative on the corresponding face of $\mathbb{R}^7_+$: ${}^C D_t^\alpha S|_{S=0} = \Lambda + \rho R \geq 0$; ${}^C D_t^\alpha E|_{E=0} = \lambda S \geq 0$; ${}^C D_t^\alpha A|_{A=0} = f_A \sigma E \geq 0$; ${}^C D_t^\alpha I|_{I=0} = f_I \sigma E \geq 0$; ${}^C D_t^\alpha I_p|_{I_p=0} = f_P \sigma E \geq 0$; ${}^C D_t^\alpha R|_{R=0} = \gamma_A A + \gamma(I + I_p) \geq 0$; and ${}^C D_t^\alpha W|_{W=0} = \alpha_A A + \alpha_1 I + \alpha_2 I_p \geq 0$. By the fractional positivity Lemma 2.4, whenever a coordinate reaches zero its Caputo derivative is non-negative, so the coordinate cannot cross into negative values; hence $\mathbb{R}^7_+$ is positively invariant. □

Theorem 3.3 (Boundedness and invariant region)**.** *The compact set*

$$\Omega = \left\{ (S, E, A, I, I_p, R, W) \in \mathbb{R}^7_+ : \; N \leq \tfrac{\Lambda}{\mu}, \; W \leq \tfrac{(\alpha_A + \alpha_1 + \alpha_2)\Lambda}{\mu \xi} \right\}$$

is positively invariant and attracting for (5)*.*

Proof. From (7), ${}^C D_t^\alpha N \leq \Lambda - \mu N$. The fractional comparison principle [31] together with the Mittag–Leffler representation of the linear bound gives $N(t) \leq N(0) E_\alpha(-\mu t^\alpha) + \frac{\Lambda}{\mu}\big(1 - E_\alpha(-\mu t^\alpha)\big)$, whence $\limsup_{t\to\infty} N(t) \leq \Lambda/\mu$ and $N(t) \leq \Lambda/\mu$ whenever $N(0) \leq \Lambda/\mu$. Since $A, I, I_p \leq N \leq \Lambda/\mu$, the water equation yields ${}^C D_t^\alpha W \leq (\alpha_A + \alpha_1 + \alpha_2)\Lambda/\mu - \xi W$, so the same argument bounds W by $(\alpha_A + \alpha_1 + \alpha_2)\Lambda/(\mu \xi)$. Therefore every trajectory enters and remains in Ω. □

The analysis below is consequently restricted to the epidemiologically meaningful region Ω.

4. Mathematical analysis

4.1. **Disease-free equilibrium and the reproduction number.**

Equilibria of the fractional system (5) solve ${}^C D_t^\alpha x = 0$, i.e. $g(x) = 0$, the *same* algebraic system as the integer-order limit, so the equilibria are independent of α. Setting the right-hand sides to zero with $E = A = I = I_p = W = 0$ yields the unique disease-free equilibrium (DFE)

$$\mathcal{E}_0 = (S^0, 0, 0, 0, 0, 0, 0), \qquad S^0 = \frac{\Lambda}{\mu} = N_0. \tag{8}$$

Because the next-generation construction is evaluated at $\mathcal{E}_0$ from the Jacobian of (5), and that Jacobian is α-independent (the α-powered constants are absorbed into the symbols), $\mathcal{R}_0$ is obtained *from the fractional system* and coincides in form with its $\alpha = 1$ limit; only the stability threshold geometry (Lemma 2.5) depends on α. Ordering the infected subsystem as (E, A, I, I_p, W), the new-infection and transition matrices at $\mathcal{E}_0$ are

$$F = \begin{pmatrix} 0 & \beta_1\varepsilon & \beta_1 & \beta_1 & \beta_2/K \\ 0 & 0 & 0 & 0 & 0 \\ 0 & 0 & 0 & 0 & 0 \\ 0 & 0 & 0 & 0 & 0 \\ 0 & \alpha_A & \alpha_1 & \alpha_2 & 0 \end{pmatrix}, \quad V = \begin{pmatrix} k_1 & 0 & 0 & 0 & 0 \\ -f_A\sigma & k_A & 0 & 0 & 0 \\ -f_I\sigma & 0 & k_2 & 0 & 0 \\ -f_P\sigma & 0 & 0 & k_3 & 0 \\ 0 & 0 & 0 & 0 & \xi \end{pmatrix}, \tag{9}$$

where $k_1 = \sigma + \mu$, $k_A = \gamma_A + \mu$, $k_2 = \gamma + \mu + \delta$, $k_3 = \gamma + \mu + \delta_p$. Shedding terms $\alpha_A A, \alpha_1 I, \alpha_2 I_p$ are placed in F so that contamination of the reservoir is treated as "infection" of W, giving the standard additive interpretation of $\mathcal{R}_0$ for waterborne pathogens [12,15]. Computing $\rho(FV^{-1})$ gives the following result.

Theorem 4.1. *The basic reproduction number of the fractional model* (5) *is*

$$\mathcal{R}_0 = \tfrac{1}{2}\Big(\mathcal{R}_d + \sqrt{\mathcal{R}_d^2 + 4\,\mathcal{R}_w}\Big), \tag{10}$$

where the direct *and* waterborne *reproduction contributions are*

$$\mathcal{R}_d = \frac{\beta_1\sigma}{k_1}\left(\frac{\varepsilon f_A}{k_A} + \frac{f_I}{k_2} + \frac{f_P}{k_3}\right), \tag{11}$$

$$\mathcal{R}_w = \frac{\beta_2}{K\xi}\cdot\frac{\sigma}{k_1}\left(\frac{\alpha_A f_A}{k_A} + \frac{\alpha_1 f_I}{k_2} + \frac{\alpha_2 f_P}{k_3}\right). \tag{12}$$

Proof. Rows two to four of F vanish, so the image of $K := FV^{-1}$ is spanned by e_E and e_W; K therefore has at most two non-zero eigenvalues, namely those of the 2×2 compression $\left(\begin{smallmatrix} a & b \\ c & 0 \end{smallmatrix}\right)$ onto $\operatorname{span}\{e_E, e_W\}$. Using the first column of V^{-1}, $(V^{-1})_{EE} = 1/k_1$, $(V^{-1})_{AE} = f_A\sigma/(k_1 k_A)$, $(V^{-1})_{IE} = f_I\sigma/(k_1 k_2)$, $(V^{-1})_{I_pE} = f_P\sigma/(k_1 k_3)$ and $(V^{-1})_{WW} = 1/\xi$, one finds $a = (K)_{EE} = \mathcal{R}_d$, $b = (K)_{EW} = \beta_2/(K\xi)$, and $c = (K)_{WE} = \frac{\sigma}{k_1}\big(\frac{\alpha_A f_A}{k_A} + \frac{\alpha_1 f_I}{k_2} + \frac{\alpha_2 f_P}{k_3}\big)$, so that $bc = \mathcal{R}_w$. The dominant eigenvalue $\frac{1}{2}(a + \sqrt{a^2 + 4bc})$ is (10). □

Remark 4.2. Equation (10) separates the two transmission pathways. The term $\mathcal{R}_d$ represents direct human transmission and includes the asymptomatic contribution $\varepsilon f_A/k_A$, whereas $\mathcal{R}_w$ represents transmission through contaminated water via pathogen shedding and ingestion. Using the baseline parameters in Table 1, we obtain $\mathcal{R}_0 \approx 2.02$, $\mathcal{R}_d \approx 1.14$, and $\mathcal{R}_w \approx 1.77$ at $\alpha = 1$, indicating that waterborne transmission is dominant, consistent with observations from the Namibian outbreak [1,2]. Under the dimensionally consistent fractional formulation, $\mathcal{R}_0$ increases with α [33,35,36]; for example, $\mathcal{R}_0 \approx 1.29$, 1.62, and 2.02 for $\alpha = 0.6$, 0.8, and 1.0, respectively. Thus, memory effects reduce the effective reproduction number while extending the epidemic duration.

4.2. **Local stability of the disease-free equilibrium.**

Theorem 4.3. *For every order $\alpha \in (0,1]$, the DFE $\mathcal{E}_0$ of the fractional system* (5) *is locally asymptotically stable if $\mathcal{R}_0 < 1$ and unstable if $\mathcal{R}_0 > 1$.*

Proof. By Lemma 2.5, $\mathcal{E}_0$ is locally asymptotically stable iff every eigenvalue λ_i of the Jacobian $J(\mathcal{E}_0)$ satisfies $|\arg(\lambda_i)| > \alpha\pi/2$. The Jacobian is block triangular: the uninfected block contributes eigenvalues $-\mu$ (twice, from S and the R–S loop, which has negative trace and positive determinant $\mu(\rho+\mu)$) and the infected block is $F - V$. Since $F \geq 0$ and V is a non-singular M-matrix, the characterisation of van den Driessche and Watmough [18] gives: all eigenvalues of $F - V$ have negative real part $\iff \mathcal{R}_0 < 1$. When $\mathcal{R}_0 < 1$, every eigenvalue of J thus has negative real part, so $|\arg(\lambda_i)| = \pi > \alpha\pi/2$ for all $\alpha \in (0, 1]$, and the Matignon condition holds. When $\mathcal{R}_0 > 1$, $F - V$ has a positive real eigenvalue $\lambda_+ > 0$ with $\arg(\lambda_+) = 0 < \alpha\pi/2$, violating (2), so $\mathcal{E}_0$ is unstable. The threshold $\mathcal{R}_0 = 1$ is therefore valid for the fractional system and, because the stability sector $\alpha\pi/2$ is wider for smaller α, the fractional DFE is "no less stable" than its integer-order counterpart. □

4.3. **Global stability of the disease-free equilibrium.**

Theorem 4.4. *If $\mathcal{R}_0 \leq 1$, the DFE $\mathcal{E}_0$ is globally asymptotically stable in Ω for the fractional system (5).*

Proof. We build a fractional Lyapunov functional. Let $\mathbf{x} = (E, A, I, I_p, W)^\top$ and let $\mathbf{w}^\top \geq 0$ be the left Perron eigenvector of $V^{-1}F$ for $\rho(V^{-1}F) = \mathcal{R}_0$. Define the linear Lyapunov function

$$L = \mathbf{w}^\top V^{-1}\mathbf{x} \geq 0, \qquad L(\mathcal{E}_0) = 0.$$

By the linearity of the Caputo operator and the comparison Lemma 2.6, and using $S \leq N$ so that the nonlinear incidence is dominated by its linearisation, $\lambda S \leq \beta_1(\varepsilon A + I + I_p) + \frac{\beta_2}{K}W$ (the water term from $W/(K+W) \leq W/K$), the infected subsystem obeys ${}^{C}D_t^{\alpha}\mathbf{x} \leq (F - V)\mathbf{x}$ componentwise. Hence

$${}^{C}D_t^{\alpha}L = \mathbf{w}^\top V^{-1}\,{}^{C}D_t^{\alpha}\mathbf{x} \leq \mathbf{w}^\top V^{-1}(F - V)\mathbf{x} = \big(\rho(V^{-1}F) - 1\big)\mathbf{w}^\top\mathbf{x} = (\mathcal{R}_0 - 1)\,\mathbf{w}^\top\mathbf{x} \leq 0$$

whenever $\mathcal{R}_0 \leq 1$. Thus ${}^{C}D_t^{\alpha}L \leq 0$ on Ω, with equality forcing $\mathbf{w}^\top\mathbf{x} = 0$, i.e. $\mathbf{x} = \mathbf{0}$ (for $\mathcal{R}_0 < 1$) or, on the largest invariant set where ${}^{C}D_t^{\alpha}L = 0$, $A = I = I_p = W = 0$, whence $S \to \Lambda/\mu$ and $R \to 0$. By the fractional Lyapunov/LaSalle theorem [31,32], $\mathcal{E}_0$ is globally asymptotically stable in Ω. □

4.4. **Endemic equilibrium.**

Theorem 4.5. *If $\mathcal{R}_0 > 1$ the fractional model (5) admits a unique endemic equilibrium $\mathcal{E}^* = (S^*, E^*, A^*, I^*, I_p^*, R^*, W^*)$ in the interior of Ω.*

Sketch. Equilibria satisfy $g(x) = 0$, independent of α. The linear chain gives $E^* = \frac{\lambda^* S^*}{k_1}$, $A^* = \frac{f_A\sigma}{k_A}E^*$, $I^* = \frac{f_I\sigma}{k_2}E^*$, $I_p^* = \frac{f_P\sigma}{k_3}E^*$, $W^* = \frac{\alpha_A A^* + \alpha_1 I^* + \alpha_2 I_p^*}{\xi}$ and $R^* = \frac{\gamma_A A^* + \gamma(I^* + I_p^*)}{\rho+\mu}$. Substituting into $\lambda^* = \beta_1(\varepsilon A^* + I^* + I_p^*)/N^* + \beta_2 W^*/(K + W^*)$ yields a single equation $g(\lambda^*) = 0$ that is continuous, has $g(0^+) > 0 \iff \mathcal{R}_0 > 1$, and is strictly decreasing on $(0, \lambda_{\max})$ because every compartment is a decreasing function of the depletion of S. Hence a unique positive root λ^* exists precisely when $\mathcal{R}_0 > 1$, determining $\mathcal{E}^*$ uniquely. □

Global stability of $\mathcal{E}^*$ for the fractional system can be established on the reduced model ($\rho = 0$) using the Volterra-type fractional Lyapunov function $U = \sum_i c_i\big(x_i - x_i^* - x_i^* \ln \frac{x_i}{x_i^*}\big)$, whose Caputo derivative obeys, by Lemma 2.6, ${}^{C}D_t^{\alpha} U \le \sum_i c_i\big(1 - \frac{x_i^*}{x_i}\big){}^{C}D_t^{\alpha} x_i \le 0$ for suitable positive weights c_i chosen by the Shuai–van den Driessche graph-theoretic method [19,31]. For the full model with waning immunity we verify global convergence numerically (Section 6), where all trajectories with $\mathcal{R}_0 > 1$ approach $\mathcal{E}^*$ irrespective of initial data and fractional order.

5. Numerical methods

The governing Caputo system (5) is solved with the Diethelm–Ford–Freed predictor–corrector (fractional Adams–Bashforth–Moulton, ABM) method [26]. For ${}^{C}D_t^{\alpha} y = f(t, y)$, $y(0) = y_0$, on a uniform grid $t_n = nh$ the corrector is

$$y_{n+1} = y_0 + \frac{h^{\alpha}}{\Gamma(\alpha+2)}\Big[f(t_{n+1}, y_{n+1}^{P}) + \sum_{j=0}^{n} a_{j,n+1} f(t_j, y_j)\Big], \tag{13}$$

with predictor $y_{n+1}^{P} = y_0 + \frac{h^{\alpha}}{\Gamma(\alpha+1)} \sum_{j=0}^{n} b_{j,n+1} f(t_j, y_j)$, $b_{j,n+1} = (n+1-j)^{\alpha} - (n-j)^{\alpha}$, and the corrector weights

$$a_{j,n+1} = \begin{cases} n^{\alpha+1} - (n-\alpha)(n+1)^{\alpha}, & j = 0, \\ (n-j+2)^{\alpha+1} + (n-j)^{\alpha+1} - 2(n-j+1)^{\alpha+1}, & 1 \le j \le n, \\ 1, & j = n+1. \end{cases} \tag{14}$$

This scheme is convergent of order $\min(2, 1+\alpha)$ and numerically stable [26,27]. The memory sum couples each step to the entire history, which is precisely the property that encodes the protracted, memory-laden enteric transmission; it also makes the cost grow as $O(n^2)$, so we use $h = 0.5$ day over horizons of up to two years.

5.1. **Integer-order check ($\alpha = 1$).** At $\alpha = 1$ the ABM scheme reduces to the classical Adams–Bashforth–Moulton method; as an independent verification we also integrate the limiting system $(5)|_{\alpha=1}$ with the explicit fourth-order Runge–Kutta (RK4) scheme,

$$\mathbf{y}_{n+1} = \mathbf{y}_n + \tfrac{h}{6}(\mathbf{k}_1 + 2\mathbf{k}_2 + 2\mathbf{k}_3 + \mathbf{k}_4), \tag{15}$$

$\mathbf{k}_1 = \mathbf{f}(t_n, \mathbf{y}_n)$, $\mathbf{k}_2 = \mathbf{f}(t_n + \frac{h}{2}, \mathbf{y}_n + \frac{h}{2}\mathbf{k}_1)$, $\mathbf{k}_3 = \mathbf{f}(t_n + \frac{h}{2}, \mathbf{y}_n + \frac{h}{2}\mathbf{k}_2)$, $\mathbf{k}_4 = \mathbf{f}(t_n + h, \mathbf{y}_n + h\mathbf{k}_3)$, with global error $O(h^4)$. The two integrators agree to plotting accuracy at $\alpha = 1$, confirming the implementation.

5.2. **Parameter estimation.** Demographic and epidemiological parameters are taken from the Namibian outbreak reports and the HEV/waterborne literature [1–3,16] and are summarised in Table 1. The natural death rate is set from a life expectancy of ≈ 64 years; the incubation (~ 40 d) and recovery (~ 30 d) periods follow clinical HEV reports [3,4]; the disease-death rates are calibrated so that the implied general and maternal case-fatality ratios reproduce the observed 0.8% and 6% [1]. The transmission coefficients β_1, β_2 are calibrated so that $\mathcal{R}_0 \approx 2.0$, matching the only published HEV outbreak estimate $(2.08–2.39$ [16]$)$. All values are illustrative of settlement conditions and are varied widely in the simulations.

5.3. **Sensitivity analysis.** The influence of each parameter θ on $\mathcal{R}_0$ is quantified by the normalized forward sensitivity index [22,23]

$$\Upsilon_\theta^{\mathcal{R}_0} = \frac{\partial \mathcal{R}_0}{\partial \theta} \cdot \frac{\theta}{\mathcal{R}_0}, \tag{16}$$

computed analytically from (10) and verified by central finite differences. A positive (negative) index means $\mathcal{R}_0$ increases (decreases) with θ. Global uncertainty is additionally explored by Latin-hypercube sampling with partial-rank correlation coefficients (LHS–PRCC) following [23]; the analytic indices and PRCC rankings agree.

6. Results and discussion

With the parameters of Table 1 the model gives, at $\alpha = 1$, $\mathcal{R}_0 \approx 2.02$. Figure 2 shows a single sharp epidemic wave: the susceptible pool is rapidly depleted, the exposed class peaks near day 22 (about 1.19×10^5), the asymptomatic and general infectious classes peak near days 43 and 50 (about 2.3×10^4 and 2.6×10^4), and almost the entire catchment transits to the recovered class, which settles near 1.90×10^5. The slow waning (ρ) sustains a small endemic tail rather than full die-out, consistent with the protracted, two-year character of the real Namibian epidemic [1]. Figure 3 separates the three infectious classes and the reservoir: the pregnant/post-partum class I_p peaks synchronously with I but at roughly 5% of its size (peak $\approx 2.8 \times 10^3$), the asymptomatic class A contributes a comparable prevalence to I, and the water compartment W rises and falls with a lag, peaking near day 69 at $\approx 4.1 \times 10^5$ and acting as the epidemic's "memory".

TABLE 1. Variables and baseline parameters (time unit: day).

Symbol	Description	Baseline	Source
S, E, A, I, I_p, R	human compartments	—	state variables
W	environmental pathogen density	—	state variable
N_0	baseline catchment population	2.0×10^5	assumed [1]
Λ	recruitment rate	μN_0	derived
μ	natural death rate	$1/(64 \times 365)$	life expectancy
β_1	direct transmission rate	0.058	calibrated ($\mathcal{R}_0 \approx 2$)
β_2	waterborne transmission rate	0.078	calibrated
ε	relative infectiousness of A	0.50	assumed [7]
K	pathogen half-saturation density	10	assumed [11]
σ	progression rate (1/incubation)	$1/40$	[3]
f_A	asymptomatic fraction of incidence	0.50	[7]
$f_P \equiv p$	pregnant fraction of incidence	0.05	assumed
f_I	general symptomatic fraction	$1 - f_A - p$	derived
γ_A	asymptomatic clearance rate	$1/20$	assumed
γ	symptomatic recovery rate	$1/30$	[4]
δ	disease death (general)	3.0×10^{-4}	CFR 0.8% [1]
δ_p	disease death (pregnant)	2.1×10^{-3}	CFR 6% [1]
ρ	waning-immunity rate	5.0×10^{-4}	assumed
α_A	shedding rate (asymptomatic)	0.40	assumed
α_1	shedding rate (general)	0.50	assumed [12]
α_2	shedding rate (pregnant)	0.50	assumed
ξ	pathogen decay/clearance rate	0.05	assumed [12]
α	Caputo fractional order	$(0, 1]$	varied

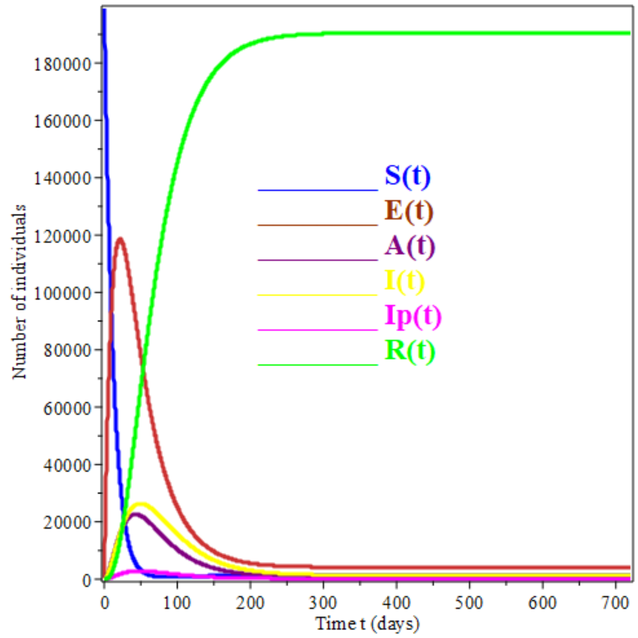

FIGURE 2. Baseline epidemic trajectories of S, E, A, I, I_p, R at $\alpha = 1$, $\mathcal{R}_0 \approx 2.02$.

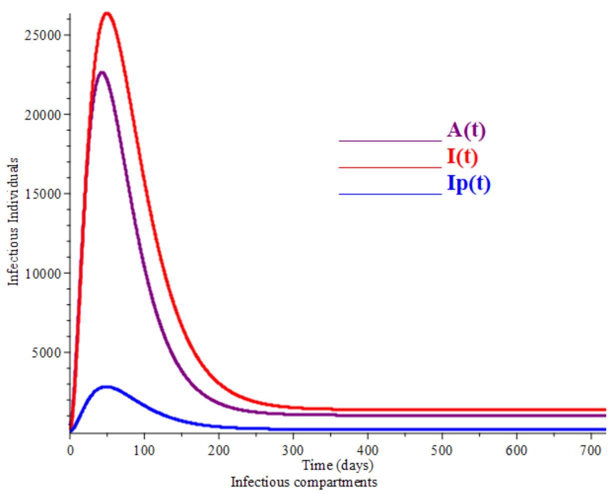

(A) Infectious classes $A(t)$, $I(t)$ and $I_p(t)$.

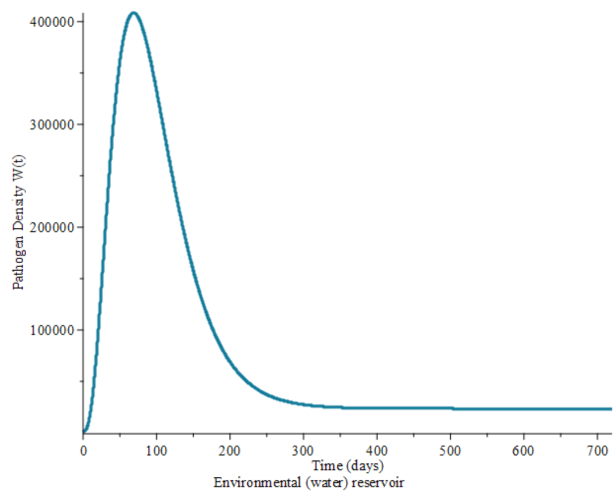

(B) Environmental pathogen density $W(t)$.

FIGURE 3. Left: asymptomatic (A), general (I), and pregnant/post-partum (I_p) infectious classes. Right: environmental pathogen density $W(t)$, which peaks after the human infectious classes and prolongs transmission.

Figures 4a and 4b vary the direct (β_1) and waterborne (β_2) transmission coefficients. To expose the comparatively weak direct pathway, the β_1 sweep in Fig. 4a is run with the waterborne route held low; under these conditions, raising β_1 from 0.020 to 0.080 increases $\mathcal{R}_0$ from 0.56 to 1.63 and amplifies the symptomatic peak from roughly 8.3×10^3 to 1.2×10^4 infectives, while only modestly shifting its timing near $t \approx 135$ days. Notably, even the sub-threshold values ($\mathcal{R}_0 < 1$) generate a transient wave seeded by the initial infectious pool before the disease settles to the low endemic floor sustained by the residual reservoir. By contrast, Fig. 4b shows that the waterborne pathway governs both the magnitude and the speed of the epidemic: eliminating it ($\beta_2 = 0$) leaves $\mathcal{R}_0 = \mathcal{R}_d \approx 1.14$ and yields an essentially flat, negligible outbreak, whereas $\beta_2 = 0.030,\ 0.078,\ 0.110$ raise $\mathcal{R}_0$ to $1.38,\ 2.02$ and 2.25 and produce sharply steeper, earlier and higher waves, the peak rising from about 2.2×10^4 near $t \approx 70$ days to 2.7×10^4 near $t \approx 45$ days. The contrast is decisive: β_1 rescales the peak by roughly one half, whereas β_2 switches the system between near-elimination and an explosive epidemic. Because $\mathcal{R}_w > \mathcal{R}_d$ at baseline, the water pathway is the principal driver: this is the quantitative expression of the field observation that the Namibian outbreak was sustained by contaminated water and open defecation in under-serviced settlements [1, 2], and it mirrors the latrine/borehole findings of the Kitgum HEV analysis [16].

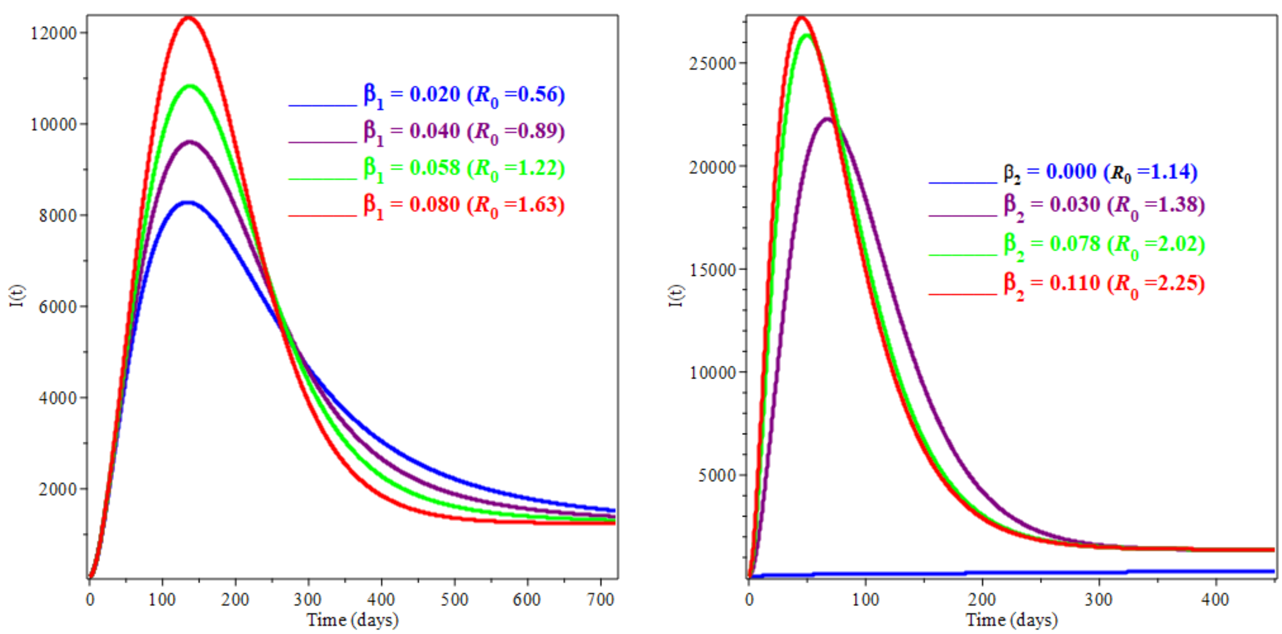

(A) Direct transmission β_1. (B) Waterborne transmission β_2.

FIGURE 4. Infectious prevalence $I(t)$ under variation of the two transmission pathways.

Figure 5 shows $I(t)$ for Caputo orders $\alpha \in \{0.70, 0.80, 0.90, 1.00\}$. As α decreases the peak prevalence falls and is delayed, and the post-peak decay slows, so that infection persists longer at lower intensity.

This memory-induced flattening is the hallmark of fractional epidemic models [35,36] and is epidemiologically appropriate for HEV, where heterogeneous environmental persistence and variable incubation create long-tailed inter-generation intervals. Under the dimensionally consistent α-powered rates, the threshold itself moves with the order — $\mathcal{R}_0 \approx 1.45, 1.62, 1.81, 2.02$ at $\alpha = 0.70, 0.80, 0.90, 1.00$ (legend of Figure 5) — so a more memory-laden process (smaller α) carries a *lower* effective reproduction number but a *longer* epidemic tail. The fractional model therefore offers a more realistic description of the slow, grinding settlement epidemics than the integer-order limit, while the $\mathcal{R}_0 = 1$ stability threshold (Theorem 4.3) remains valid for every α via the Matignon criterion.

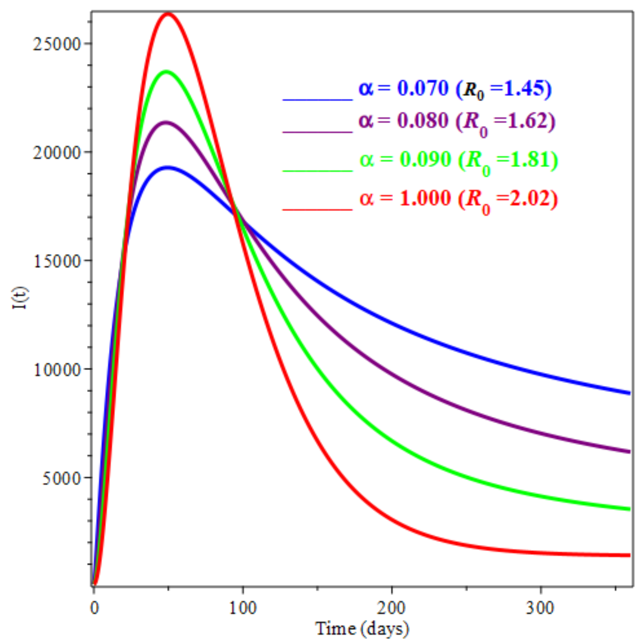

FIGURE 5. Caputo-fractional memory effect.

Table 2 and Figure 6 report the normalized sensitivity indices of $\mathcal{R}_0$. The symptomatic recovery rate γ is the most influential ($\Upsilon = -0.48$): faster recovery (earlier isolation, supportive care) sharply reduces transmission. Among controllable drivers, the direct rate β_1 $(+0.39)$, the waterborne rate β_2 $(+0.30)$, the asymptomatic fraction f_A (-0.29), the pathogen half-saturation K (-0.30) and the environmental decay ξ (-0.30) carry the largest weight. The equal-magnitude indices of β_2, K and ξ follow directly from (10), since they enter only through $\mathcal{R}_w \propto \beta_2/(K\xi)$. The negative index of f_A reflects that diverting incident infections into the faster-clearing, lower-shedding asymptomatic stream lowers $\mathcal{R}_0$; nonetheless asymptomatic shedding still contributes positively through α_A $(+0.11)$ and ε $(+0.10)$. Practically, a 10% improvement in water treatment (raising ξ or K) lowers $\mathcal{R}_0$ by about 3%, of the same order as a 10% cut in the direct transmission coefficient.

Figure 7 compares four strategies against symptomatic infectious prevalence $I + I_p$, and Figure 8 tracks the maternal class I_p. A WASH package that cuts waterborne transmission by 60% and accelerates

TABLE 2. Normalized forward sensitivity indices of $\mathcal{R}_0$ ($\Upsilon_\theta^{\mathcal{R}_0}$), ranked by magnitude. Baseline $\mathcal{R}_0 \approx 2.02$.

Parameter	Index	Parameter	Index
γ	-0.484	α_A	$+0.106$
β_1	$+0.395$	ε	$+0.100$
β_2	$+0.303$	α_2	$+0.019$
ξ	-0.303	δ_p	-0.003
K	-0.303	p	-0.003
f_A	-0.288	μ	-0.002
γ_A	-0.206	σ	$+0.001$
α_1	$+0.178$		

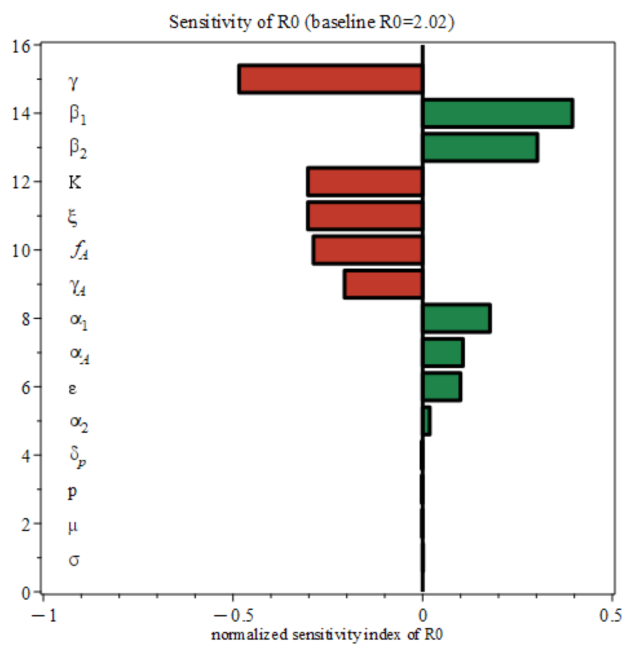

FIGURE 6. Tornado plot of the $\mathcal{R}_0$ sensitivity indices. Green: $\mathcal{R}_0$ increases with the parameter; red: $\mathcal{R}_0$ decreases.

pathogen clearance by 50% lowers $\mathcal{R}_0$ to 1.47; a hygiene-promotion package halving direct transmission lowers it to 1.65; and the *combined* package brings $\mathcal{R}_0$ to ≈ 1.03, essentially the elimination threshold. The combined strategy lowers the symptomatic peak from $\approx 2.9 \times 10^4$ to $\approx 2.4 \times 10^4$ and delays it from day 50 to day 67, and lowers peak maternal prevalence from $\approx 2.8 \times 10^3$ to $\approx 2.3 \times 10^3$.

A modelling subtlety carries a sharp policy message. Because the saturating water response reaches near-maximal infectiousness at a low pathogen density K, once an outbreak is underway the reservoir is effectively saturated ($W \gg K$) and the waterborne force of infection sits near its ceiling β_2. Partial water improvements then mainly *flatten and delay* the wave rather than abort it; the cumulative two-year maternal burden falls only modestly until the intervention is strong enough to drive $\mathcal{R}_0$ below 1 and re-stabilise the disease-free state (Theorem 4.4). For Namibia this argues against incremental, piecemeal water measures and in favour of decisive decontamination that crosses the threshold. Three policy messages follow.

(1) **Environmental decontamination must lead, and must be decisive.** Because $\mathcal{R}_w > \mathcal{R}_d$ and β_2, K, ξ are jointly more influential than the direct route, expanding piped water, communal ablution and sewerage in Havana, Goreangab and comparable settlements is the highest-leverage action — but only sustained, threshold-crossing investment converts delay into prevention [1,2].

(2) **Hygiene promotion is complementary, not sufficient.** Halving β_1 alone leaves $\mathcal{R}_0 > 1$; only the combined strategy approaches the threshold, so hand-hygiene campaigns must accompany — not replace — infrastructure.

(3) **Protect pregnant women explicitly.** Even at equal prevalence the elevated δ_p concentrates mortality in I_p; antenatal screening, prioritised clean-water access and early referral for jaundiced pregnant women would cut deaths faster than the prevalence reduction alone [1,5].

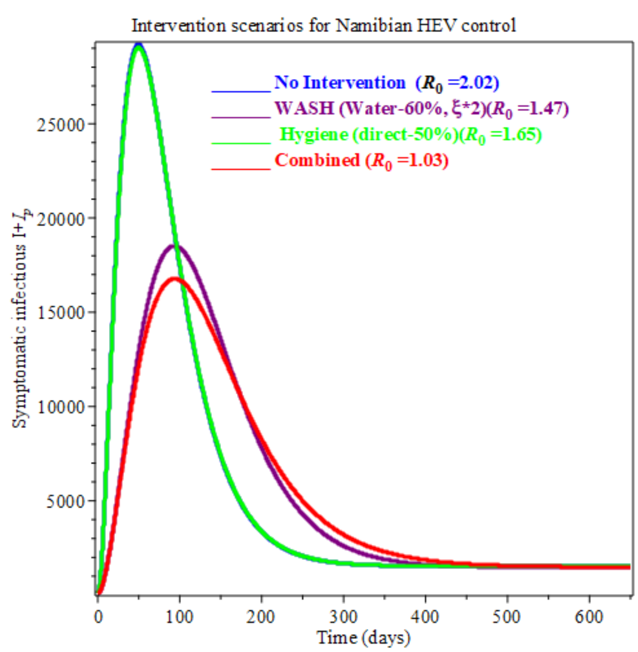

FIGURE 7. Symptomatic infectious prevalence $I + I_p$ under control scenarios. The combined WASH+hygiene strategy drives $\mathcal{R}_0$ to ≈ 1.03, flattening and delaying the peak.

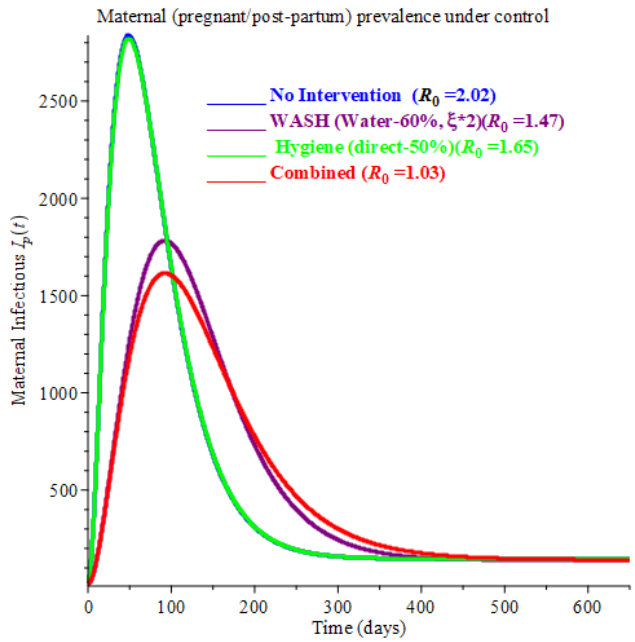

FIGURE 8. Maternal (pregnant/post-partum) infectious prevalence $I_p(t)$ under the same scenarios; control lowers and delays the maternal peak, but only threshold-crossing strategies ($\mathcal{R}_0 < 1$) prevent rather than postpone the burden.

Comparison with previous studies. Our baseline $\mathcal{R}_0 \approx 2.02$ is consistent with the only comparable HEV estimate, 2.08–2.39 for Kitgum, Uganda [16], and with the reproduction numbers reported for analogous waterborne cholera epidemics [14,15]. Unlike those models, ours (i) is tailored to Namibia, (ii) resolves maternal risk through the I_p class and subclinical transmission through the asymptomatic class A, and (iii) provides a closed-form additive decomposition of $\mathcal{R}_0$ into direct and waterborne loops that maps onto specific interventions. The dominance of the environmental pathway echoes Tien and Earn's general finding that the water compartment governs the long-time dynamics of waterborne pathogens [12,13].

Limitations. The model is deterministic and assumes a well-mixed catchment, omitting spatial structure across the 14 regions and seasonality (the rainy season elevates surface-water use [2]). Parameters are calibrated rather than formally fitted, owing to the aggregated nature of the surveillance data; a formal Bayesian fit to the weekly case series, together with practical identifiability of β_1 versus β_2 [13], is left for future work. The saturating (Holling type II) water response, with a low half-saturation K, implies that the reservoir is near-saturated during active transmission, so the model is most informative about thresholds and timing rather than the fine cumulative toll of partial interventions; a dose–response calibration of K against measured environmental loads would sharpen the intervention projections. Age structure is also not resolved explicitly.

7. Conclusion

We have developed the first mechanistic transmission model of the Namibian hepatitis E epidemic: a seven-compartment S–E–A–I–I_p–R–W system with a saturating waterborne pathway, an explicit asymptomatic shedding class and an explicit pregnant/post-partum class, formulated directly as a Caputo fractional system of order $\alpha \in (0, 1]$ (the integer-order model being the limit $\alpha \to 1$). Working throughout on the fractional system, we proved positivity, boundedness and a positively invariant region; derived the basic reproduction number from the next-generation matrix at the fractional disease-free equilibrium, in closed form splitting additively into direct and waterborne contributions; and established local stability via the Matignon argument-criterion and global stability via a fractional Lyapunov construction, together with the existence and uniqueness of an endemic equilibrium. Numerically, the model reproduces a realistic settlement epidemic with $\mathcal{R}_0 \approx 2.02$ dominated by the waterborne loop ($\mathcal{R}_w \approx 1.77$ versus $\mathcal{R}_d \approx 1.14$); the fractional order modulates both the peak and the effective $\mathcal{R}_0$ through memory; and sensitivity analysis identifies recovery, the two transmission rates, the asymptomatic fraction, and the environmental parameters K and ξ as the key levers. We note that the normalized $\mathcal{R}_0$-sensitivity, computed at the disease-free equilibrium where the reservoir term is unsaturated, attributes substantial weight to β_1; in the saturated endemic regime, however, the realized epidemic is governed by β_2, which is why hygiene measures targeting β_1 must complement rather than lead environmental control. The central contribution is both mathematical — a tractable additive $\mathcal{R}_0$ and a fully fractional stability theory for a dual-pathway, maternal-stratified waterborne model with asymptomatic shedding — and practical: for Namibia, environmental decontamination must lead the response, hygiene promotion must complement it, and pregnant women require targeted protection. A combined WASH-plus-hygiene strategy pushes $\mathcal{R}_0$ to the elimination threshold and flattens and delays the epidemic; because the reservoir saturates at low pathogen density, only threshold-crossing decontamination converts that delay into durable prevention. Future research will fit the model to the regional weekly case series, add spatial and seasonal structure, incorporate optimal-control and cost-effectiveness analysis of WASH investment, and explore alternative non-singular fractional kernels [34].according to the numerical results that we obtained. whereas the exposed, careless infective, and careful infective compartments are reduced by treatment rates $\phi_1$and ϕ_2, respectively.

Authors' Contributions. All authors have read and approved the final version of the manuscript. The authors contributed equally to this work.

Conflicts of Interest. The authors declare that there are no conflicts of interest regarding the publication of this paper.

References

[1] N.D. Bustamante, S.R. Matyenyika, L.A. Miller, M. Goers, P. Katjiuanjo, et al., Notes from the Field: Nationwide Hepatitis E Outbreak Concentrated in Informal Settlements — Namibia, 2017–2020, MMWR Morb. Mortal. Wkly. Rep. 69 (2020), 355–357. https://doi.org/10.15585/mmwr.mm6912a6.

[2] World Health Organization, Hepatitis E — Namibia, Disease Outbreak News, 15 January 2018. https://www.who.int/emergencies/disease-outbreak-news/item/15-january-2018-hepatitis-e-namibia-en.

[3] N. Kamar, J. Izopet, N. Pavio, R. Aggarwal, A. Labrique, et al., Hepatitis E Virus Infection, Nat. Rev. Dis. Primers 3 (2017), 17086. https://doi.org/10.1038/nrdp.2017.86.

[4] R. Aggarwal, S. Naik, Epidemiology of Hepatitis E: Current Status, J. Gastroenterol. Hepatol. 24 (2009), 1484–1493. https://doi.org/10.1111/j.1440-1746.2009.05933.x.

[5] M.T. Pérez-Gracia, B. Suay-García, M.L. Mateos-Lindemann, Hepatitis E and Pregnancy: Current State, Rev. Med. Virol. 27 (2017), e1929. https://doi.org/10.1002/rmv.1929.

[6] D.B. Rein, G.A. Stevens, J. Theaker, J.S. Wittenborn, S.T. Wiersma, The Global Burden of Hepatitis E Virus Genotypes 1 and 2 in 2005, Hepatology 55 (2012), 988–997. https://doi.org/10.1002/hep.25505.

[7] B. Kmush, T. Wierzba, L. Krain, K. Nelson, A. Labrique, Epidemiology of Hepatitis E in Low- and Middle-Income Countries of Asia and Africa, Semin. Liver Dis. 33 (2013), 015–029. https://doi.org/10.1055/s-0033-1338111.

[8] World Health Organization, Hepatitis E Vaccine: WHO Position Paper, May 2015, Wkly. Epidemiol. Rec. 90 (2015), 185–200. https://www.who.int/publications-detail-redirect/WER9018-185-200.

[9] H.W. Hethcote, The Mathematics of Infectious Diseases, SIAM Rev. 42 (2000), 599–653. https://doi.org/10.1137/s0036144500371907.

[10] O. Diekmann, J.A.P. Heesterbeek, J.A.J. Metz, On the Definition and the Computation of the Basic Reproduction Ratio R_0 in Models for Infectious Diseases in Heterogeneous Populations, J. Math. Biol. 28 (1990), 365–382. https://doi.org/10.1007/bf00178324.

[11] C.T. Codeço, Endemic and Epidemic Dynamics of Cholera: the Role of the Aquatic Reservoir, BMC Infect. Dis. 1 (2001), 1. https://doi.org/10.1186/1471-2334-1-1.

[12] J.H. Tien, D.J.D. Earn, Multiple Transmission Pathways and Disease Dynamics in a Waterborne Pathogen Model, Bull. Math. Biol. 72 (2010), 1506–1533. https://doi.org/10.1007/s11538-010-9507-6.

[13] M.C. Eisenberg, S.L. Robertson, J.H. Tien, Identifiability and Estimation of Multiple Transmission Pathways in Cholera and Waterborne Disease, J. Theor. Biol. 324 (2013), 84–102. https://doi.org/10.1016/j.jtbi.2012.12.021.

[14] A.R. Tuite, J. Tien, M. Eisenberg, D.J.D. Earn, J. Ma, et al., Cholera Epidemic in Haiti, 2010: Using a Transmission Model to Explain Spatial Spread of Disease and Identify Optimal Control Interventions, Ann. Intern. Med. 154 (2011), 593–601. https://doi.org/10.7326/0003-4819-154-9-201105030-00334.

[15] Z. Mukandavire, S. Liao, J. Wang, H. Gaff, D.L. Smith, J.G. Morris, et al., Estimating the Reproductive Numbers for the 2008–2009 Cholera Outbreaks in Zimbabwe, in: Proceedings of the National Academy of Sciences, National Academy of Sciences, 2011, pp. 8767–8772. https://doi.org/10.1073/pnas.1019712108.

[16] B. Nannyonga, D.J.T. Sumpter, J.Y.T. Mugisha, L.S. Luboobi, The Dynamics, Causes and Possible Prevention of Hepatitis E Outbreaks, PLoS One 7 (2012), e41135. https://doi.org/10.1371/journal.pone.0041135.

[17] H. Ren, J. Li, Z. Yuan, J. Hu, Y. Yu, et al., The Development of a Combined Mathematical Model to Forecast the Incidence of Hepatitis E in Shanghai, China, BMC Infect. Dis. 13 (2013), 421. https://doi.org/10.1186/1471-2334-13-421.

[18] P. van den Driessche, J. Watmough, Reproduction Numbers and Sub-threshold Endemic Equilibria for Compartmental Models of Disease Transmission, Math. Biosci. 180 (2002), 29–48. https://doi.org/10.1016/s0025-5564(02)00108-6.

[19] Z. Shuai, P. van den Driessche, Global Stability of Infectious Disease Models Using Lyapunov Functions, SIAM J. Appl. Math. 73 (2013), 1513–1532. https://doi.org/10.1137/120876642.

[20] J.P. La Salle, The Stability of Dynamical Systems, SIAM, 1976. https://doi.org/10.1137/1.9781611970432.

[21] C. Castillo-Chavez, B. Song, Dynamical Models of Tuberculosis and Their Applications, Math. Biosci. Eng. 1 (2004), 361–404. https://doi.org/10.3934/mbe.2004.1.361.

[22] N. Chitnis, J.M. Hyman, J.M. Cushing, Determining Important Parameters in the Spread of Malaria Through the Sensitivity Analysis of a Mathematical Model, Bull. Math. Biol. 70 (2008), 1272–1296. https://doi.org/10.1007/s11538-008-9299-0.

[23] S. Marino, I.B. Hogue, C.J. Ray, D.E. Kirschner, A Methodology for Performing Global Uncertainty and Sensitivity Analysis in Systems Biology, J. Theor. Biol. 254 (2008), 178–196. https://doi.org/10.1016/j.jtbi.2008.04.011.

[24] M. Caputo, Linear Models of Dissipation whose Q is Almost Frequency Independent—II, Geophys. J. R. Astron. Soc. 13 (1967), 529–539. https://doi.org/10.1111/j.1365-246x.1967.tb02303.x.

[25] I. Podlubny, Fractional Differential Equations, Mathematics in Science and Engineering, vol. 198, Academic Press, San Diego, 1999.

[26] K. Diethelm, N.J. Ford, A.D. Freed, A Predictor-Corrector Approach for the Numerical Solution of Fractional Differential Equations, Nonlinear Dyn. 29 (2002), 3–22. https://doi.org/10.1023/a:1016592219341.

[27] K. Diethelm, N.J. Ford, Analysis of Fractional Differential Equations, J. Math. Anal. Appl. 265 (2002), 229–248. https://doi.org/10.1006/jmaa.2000.7194.

[28] D. Matignon, Stability Results for Fractional Differential Equations with Applications to Control Processing, in: Computational Engineering in Systems Applications, IMACS, Lille, pp. 963–968, 1996.

[29] A.S. Eegunjobi, Modelling the Dynamics of Tuberculosis: a Multi-Stage Compartmental Approach, J. Math. Fundam. Sci. 57 (2025), 146–172. https://doi.org/10.5614/j.math.fund.sci.2025.57.2.5.

[30] I. Petráš, Fractional-Order Nonlinear Systems: Modeling, Analysis and Simulation, Springer Berlin Heidelberg, 2011. https://doi.org/10.1007/978-3-642-18101-6.

[31] C. Vargas-De-León, Volterra-Type Lyapunov Functions for Fractional-Order Epidemic Systems, Commun. Nonlinear Sci. Numer. Simul. 24 (2015), 75–85. https://doi.org/10.1016/j.cnsns.2014.12.013.

[32] H. Delavari, D. Baleanu, J. Sadati, Stability Analysis of Caputo Fractional-Order Nonlinear Systems Revisited, Nonlinear Dyn. 67 (2012), 2433–2439. https://doi.org/10.1007/s11071-011-0157-5.

[33] K. Diethelm, A Fractional Calculus Based Model for the Simulation of an Outbreak of Dengue Fever, Nonlinear Dyn. 71 (2013), 613–619. https://doi.org/10.1007/s11071-012-0475-2.

[34] A. Atangana, D. Baleanu, New Fractional Derivatives with Nonlocal and Non-singular Kernel: Theory and Application to Heat Transfer Model, Therm. Sci. 20 (2016), 763–769. https://doi.org/10.2298/tsci160111018a.

[35] S. Osman, B.S. Lassong, M. Dasumani, E.Y. Boateng, W.M. Onsongo, et al., Modeling the Transmission Routes of Hepatitis E Virus as a Zoonotic Disease Using Fractional-Order Derivative, J. Appl. Math. 2024 (2024), 5168873. https://doi.org/10.1155/2024/5168873.

[36] S. Chakraverty, R.M. Jena, S.K. Jena, Time-Fractional Model of Hepatitis E Virus with Uncertain Parameters, in: Time-Fractional Order Biological Systems with Uncertain Parameters, Synthesis Lectures on Mathematics and Statistics, Springer, Cham, pp. 105–122, (2020). https://doi.org/10.1007/978-3-031-02423-8_7.

[37] A.S. Eegunjobi, N. Chere, D. Iiyambo, P.M. Ndeevelo, Mathematical Analysis of FMD with Optimal Control, Asia Pac. J. Math. 12 (2025), 42. https://doi.org/10.28924/apjm/12-42.